Published in final edited form as:
Opt Lett. 2009 October 15; 34(20): 3235–3237.

Line-Scanning Reflectance Confocal Microscopy of Human Skin: Comparison of Full-pupil and Divided-pupil Configurations

Daniel S. Gareau, **Sanjee Abeytunge**, and **Milind Rajadhyaksha**
Memorial Sloan-Kettering Cancer Center, Dermatology Service, 160 East 53rd Street, New York, NY 10022

Abstract

Line-scanning, with pupil engineering and the use of linear array detectors, may enable simple, small and low-cost confocal microscopes for clinical imaging of human epithelial tissues. However, a fundamental understanding of line-scanning performance within the highly scattering and aberrating conditions of human tissue is necessary, to translate from benchtop instrumentation to clinical implementation. The results of a preliminary investigation for reflectance imaging in skin are reported.

Point-scanning confocal microscopes are well-proven for optical sectioning and imaging of nuclear and cellular detail in human skin [1]. However, line-scanning is fundamentally simpler, and the recent advent of high-quality linear array detectors may enable smaller and lower-cost confocal microscopy [2–4]. Scanning only once, directly behind the pupil of the objective lens, and de-scanning once, directly onto a linear array detector, allows considerable simplification of the original confocal line-scanning designs.

Of particular clinical importance is imaging performance with reflectance as an endogenous source of contrast, in highly scattering and aberrating human tissues. A fundamental understanding of confocal line-scanning performance in human tissue is therefore a necessary translational bridge from benchtop instrumentation to clinical implementation. For such investigations, the epidermis in human skin is easily accessible and available, and is an excellent model for the scattering and aberrating properties of epithelial tissue. In this Letter, we present a full-pupil line-scanning confocal microscope, and comparison of its performance to a divided-pupil configuration, for reflectance imaging of nuclear and cellular morphology in human epidermis, both *in vivo* and *ex vivo*.

As in the divided-pupil design that we reported earlier [5,6], the full-pupil line-scanning microscope, too, consists of 8–10 optical components in a simple configuration, with total hardware costs of $15,000. The electronics is based on field programmable gate array (FPGA) logic. The development of FPGA-based electronics offers the advantages of small footprint, rapid reconfigurability and complete integration toward a stand-alone system. In the long-term, line-scanning with the use of FPGA-based electronics may enable simple, small, low-cost stand-alone confocal microscopes for use at-the-bedside in diverse healthcare settings worldwide.

Figure 1 shows the full-pupil line-scanning confocal microscope. A collimated beam is incident on a cylindrical lens (L_{cyl}), which is placed so as to produce a focused line in the back focal plane (BFP) of an objective lens (Obj). The focused line in the BFP is Fourier-transformed or re-focused to a line that is oriented perpendicular to the axis of the cylindrical lens. This produces a focused line in the object plane (within tissue) that is oriented perpendicular to the plane of this page. The line is scanned by an oscillating galvanometrically-driven scan mirror (G). The scan mirror is placed as close as possible to the pupil of the objective lens. No relay

telescopes are used such that assembly, alignment, testing and troubleshooting is reasonably easy. However, the scanning does not occur exactly in the pupil of the objective lens. Thus, the focused line dithers across the pupil. Vignetting at the edges of the scan is minimized by overfilling the pupil. The line is ~10 mm in length, with dither of ±0.9 mm, relative to pupil diameter of ~7 mm. The light that is back-scattered from the object plane is relayed, de-scanned and focused by a spherical lens (Ld) onto a linear charge coupled-device (CCD) array detector. When imaging, the linear array detector, itself, acts as a detection slit aperture, with 14x14 μm-pixels that correspond to sub-diffraction resolution and almost satisfy Nyquist's sampling condition. The magnification in the detection optics almost satisfies the Nyquist requirement but results in the detected line underfilling the linear array detector by about 11% at the edges. This, along with an estimated 60% illumination fall-off due to the Gaussian beam profile causes the edges of the image, in the non-scanned direction, to appear dark.

The video timing, control and synchronization signals are based on an FPGA (Altera-Cyclone, San Jose, CA). Images are acquired with a frame grabber (Imaq PCI-1410, National Instruments, Austin, TX). The linear CCD detector (LC3022, Perkin Elmer) consists of a linear photodiode array (Reticon RL1024P, Perkin Elmer) and operates at a maximum clock frequency of 20 MHz, allowing acquisition of images consisting of 1024 pixels×1024 lines with 8 bit grayscale resolution, at a maximum rate of 20 frames per second. We calculate the sensitivity to be ~10^8 Volts/Watt. The specified dynamic range of ~2500 (~68 dB) is sufficient for imaging human skin.

With illumination power of 20–100 μW/pixel (i. e., 20–100 mW/line) on skin, the detected power is estimated to be ~4,000–20,000 photons/pixel in the linear array detector. The calculated root-mean-square (RMS) quantum noise is ~57–179 electrons, while the specified RMS read-out noise is ~50 electrons and dark noise is ~52 electrons. Thus, the RMS signal-to-noise ratio (SNR) is estimated to be ~35–82. The SNR can be quantum noise-limited when the illumination power is high. However, in practice, dark noise and read-out noise is significant when there is loss of illumination power, especially when imaging deeper in tissue.

The nominal FWHM optical section in line-scanning is 20% thicker than that with point-scanning [7] and is given by $1.14n\lambda/NA^2$ (i. e., 1.55 μm) when measured with a plane object, where n is the refractive index (i. e., 1.33) of the immersion medium, λ is the illumination wavelength (i. e., 830 nm) and NA is the numerical aperture (i. e., 0.9) of the objective lens. Optical sectioning was experimentally evaluated in terms of the FWHM of axial line-spread functions (LSFs), using a λ/20-flat mirror and a 25μm-slit aperture in front of a photodiode detector. The procedure was described earlier [5,6]. The slit width of 25 μm corresponds to slightly larger than the diffraction-limited lateral resolution. Measurements with the mirror were of the optical section thickness under nominal conditions. To further understand the effects of tissue-induced scattering and aberrations, measurements of LSF were also performed through an overlying layer of full-thickness human epidermis on the mirror surface. Human epidermis specimens, of measured thicknesses ~50–75 μm, were harvested from discarded surgical skin excisions under an IRB-approved protocol. Five measurements of optical section thickness were performed.

The nominal FWHM lateral resolution is 0.61λ/NA (i. e., 0.56 μm) in the confocal and 0.79λ/NA (i. e., 0.73 μm) in the non-confocal direction. Lateral resolution was experimentally evaluated in terms of the FWHM of edge spread functions (ESFs), from images of a Ronchi ruling target. The FWHM lateral resolution is determined from the measured 10–90% width of the ESF. The method was detailed earlier [5,6]. The lateral resolution was measured, again, under nominal conditions as well as through an overlying layer of full-thickness human epidermis on the Ronchi ruling target. Five measurements of lateral resolution were performed.

Figure 2 shows examples of measured axial LSFs, lateral ESFs, lateral LSFs obtained as derivatives of the ESFs, and images of an edge in a Ronchi ruling target, both under nominal conditions and through the scattering and aberrating conditions of full-thickness human epidermis. Table 1 shows the measured values for FWHM optical section thickness and lateral resolution for the full-pupil line-scanning confocal microscope. For comparison, also included are previous measurements with our divided-pupil configuration [5,6].

The nominal FWHM optical sectioning, when imaging in the superficial epidermis, is comparable for both pupil configurations. However, through the epidermis, when imaging in the underlying deeper dermis, the degradation is less than 2-fold for the full-pupil but more than 5-fold for the divided-pupil. The higher difference and variability in optical sectioning with the divided-pupil configuration is due to the separate illumination and detection paths (which mimics the well-known theta microscope geometry [8]). With separate paths, the overlying heterogeneous epidermis and dermo-epidermal junction produces spatially varying mismatches between the illumination and detection LSFs and loss of peak irradiance in the focal plane in the underlying deeper dermis. By comparison, the coaxial illumination and detection paths in the full-pupil configuration result in the LSF being less sensitive to the overlying epidermis and dermo-epidermal junction.

The difference and variability in lateral resolution is comparatively smaller. The diffraction-limited FWHM lateral resolution with a confocal microscope is only 30% better than that with a conventional microscope [7]. In practice, this marginal improvement usually degrades due to detection aperture size, instrumental imperfections and tissue-induced scattering and aberrations, such that the two pupil configurations offer somewhat comparable lateral resolution.

Figure 3 shows images of human skin, both *in vivo* and *ex vivo*, with both full-pupil and divided-pupil line-scanning confocal microscopes. The images confirm that the measured nominal FWHM optical sectioning and lateral resolution are comparable for the full-pupil and divided-pupil configurations, and adequate for visualizing nuclear and cellular detail in the epidermis. Both out-of-focus multiply scattered background light and speckle noise is evident in the images. The visually-assessed contrast is lower and the images somewhat more noisy with the full-pupil configuration than that seen earlier [5,6] with our divided-pupil configuration. The rejection of background light in the epidermis is stronger and the resulting image contrast superior with the divided-pupil configuration, due to the angular separation of the detection path from the illumination path. Within dark nuclei, intra-nuclear structure is often distinctly noticeable, which is not seen with the full-pupil configuration. However, as noted in Table 1, through epidermis and when deeper in the underlying dermis, the full-pupil configuration provides significantly better optical sectioning with less tissue-induced variability.

In conclusion, line-scanning confocal microscopy may offer a competitive alternative to current point-scanning technology for imaging nuclear detail in epithelial tissues for clinical utility. The full-pupil configuration is easier to implement than the divided-pupil. However, the choice of pupil configuration and the trade-offs in optical sectioning, resolution and contrast will depend on the scattering and aberrating properties of tissue for any desired clinical application.

Acknowledgments

This research was supported by NIH grant EB006947 from the NIBIB.

References

1. Gonzalez, SG.; Gill, M.; Halpern, AC., editors. Reflectance Confocal Microscopy of Cutaneous Tumors – An Atlas with Clinical, Dermoscopic and Histological Correlations. London: Informa Healthcare; 2008.
2. Im K-B, Han S, Park H, Kim D, Kim B-M. Simple high-speed confocal line-scanning microscope. Optics Express 2005;13:5151–5156. [PubMed: 19498504]
3. Wolleschensky R, Zimmerman B, Kempe M. High-speed confocal fluorescence imaging with a novel line scanning microscope. J. Biomed. Optics 2006;11:064011.
4. Hammer DX, Ferguson RD, Ustun TE, Bigelow CE, Iftimia NV, Webb RH. Line-scanning ophthalmoscope. J. Biomed. Optics 2006;11:041126.
5. Dwyer PJ, DiMarzio CA, Zavislan JM, Fox WJ, Rajadhyaksha M. Confocal reflectance theta line-scanning microscope for imaging human skin *in vivo*. Optics Letters 2006;31:942–944. [PubMed: 16599219]
6. Dwyer PJ, DiMarzio CA, Rajadhyaksha M. Confocal theta line-scanning microscope for imaging human tissues. Applied Optics 2007;46:1843–1851. [PubMed: 17356629]
7. Wilson, T., editor. Confocal Microscopy. New York: Academic Press; 1990.
8. Stelzer EHK, Lindek S. Fundamental reduction of the observed volume in far-field light microscopy by detection orthogonal to the illumination axis: Confocal theta microscopy. Opt. Commun 1994;111:536–547.

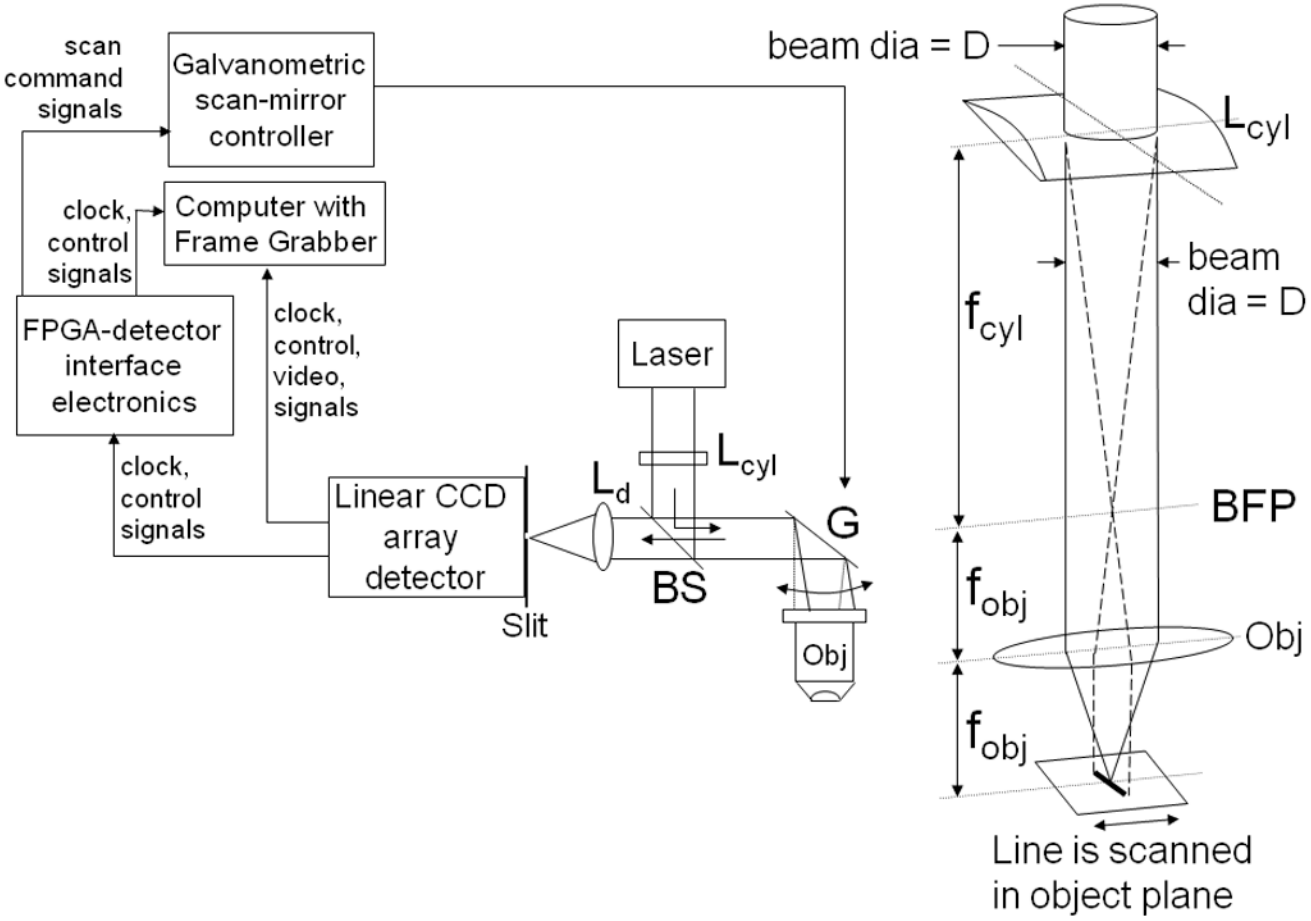

Figure 1.

The full-pupil line-scanning confocal microscope. Illumination is with a collimated beam of diameter ~10 mm from a diode laser at the near infrared wavelength of 830 nm (L4 830S-115-TE/ESYS, Microlaser Inc.). The illumination path includes a cylindrical lens (L_{cyl}) of focal length f_{cyl} = 100 mm, a 50/50 thin plate beamsplitter (BS), a galvanometric scan mirror (G, MiniSAX, GSI Lumonics) and a water immersion objective lens (Obj., Olympus 60X, 0.9 NA) of focal length f_{obj} = 4 mm. The detection path includes a spherical detector lens (L_d) of focal length f_d = 160 mm and a linear CCD array detector (Reticon LC3022 with photodiode RL1024P Perkin-Elmer, Canada). The magnification in the detection path is f_d/f_{obj} = 40X.

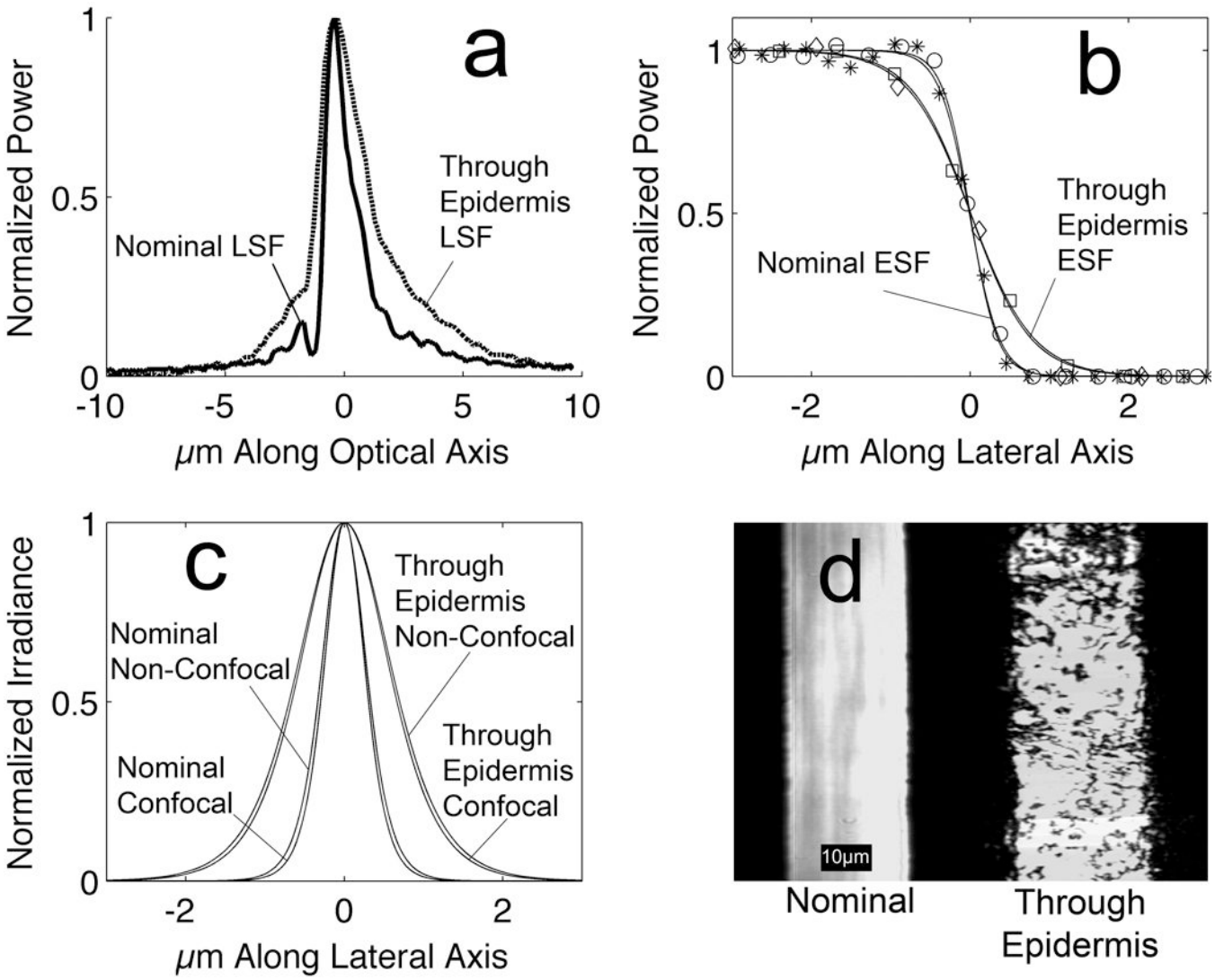

Figure 2.

Experimentally measured axial LSFs (a), lateral ESFs (b) and lateral LSFs (c) under both nominal conditions and through full-thickness human epidermis. The 10–90% width of the ESFs is determined by approximating with sigmoidal fits. Images of an edge in a reflective chrome-on-glass Ronchi ruling target, showing, visually, the nominal resolution and the degradation through epidermis (d).

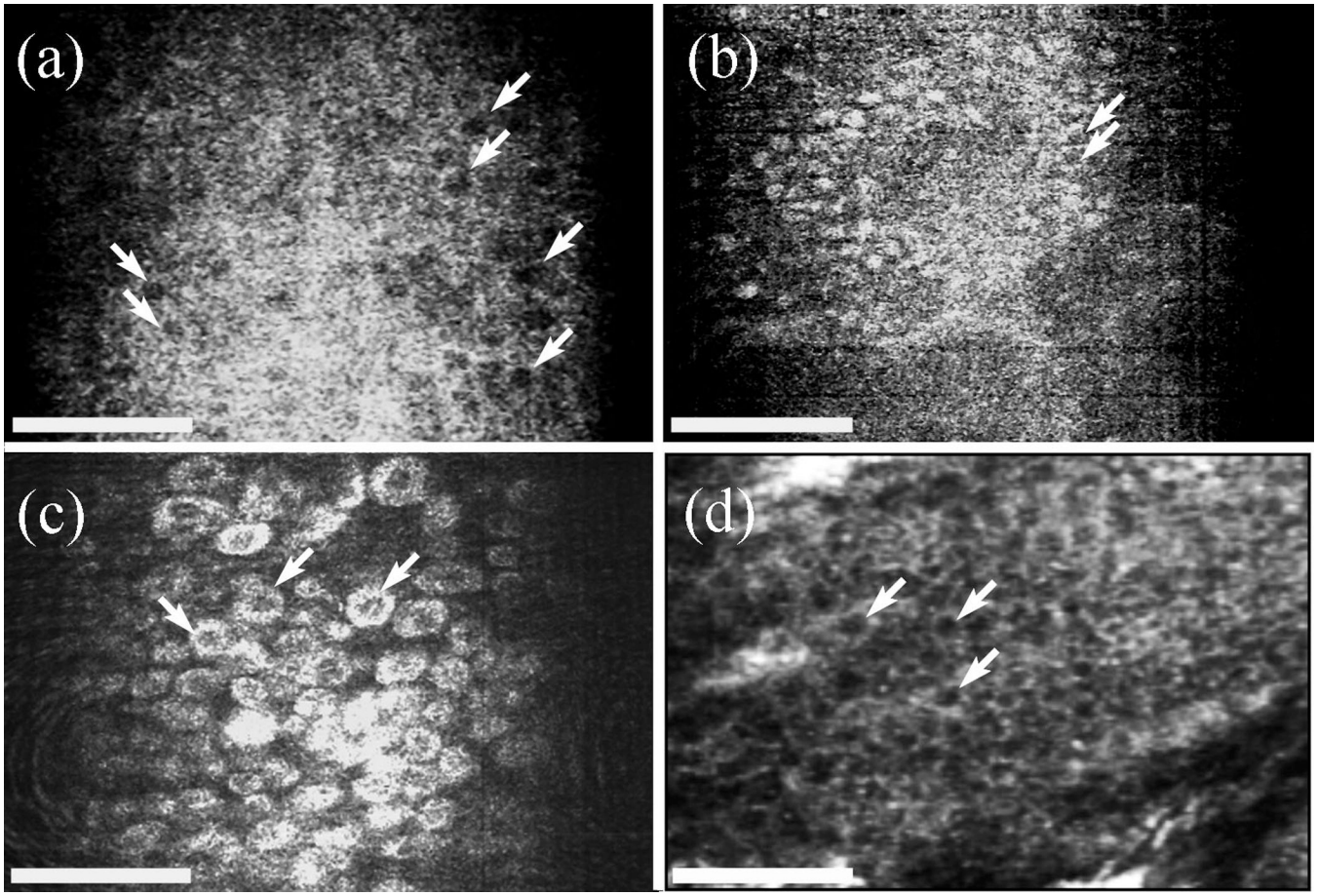

Figure 3.
Reflectance images of human epidermis with the full-pupil line-scanning confocal microscope (a–c). Dark-appearing nuclei are seen within bright and grainy cellular cytoplasm (arrows) in the spinous layers *in vivo* at depths of ~20–50 μm (a) and basal layer *in vivo* at depths of ~50–100 μm (b), and in superficial layers of surgically excised skin *ex vivo* (c). Also shown is an earlier image of the spinous layer *in vivo* with the previously reported divided-pupil configuration (d). Scale bar 75 μm.

Table 1

The measured values of FWHM optical section thickness and confocal lateral resolution for full-pupil and divided-pupil configurations. For the full-pupil configuration, lateral resolution in the non-confocal direction is nominally 0.9 μm and 1.6 μm through full-thickness epidermis.

Measured parameter		Full-pupil configuration	Divided-pupil configuration
FWHM optical section thickness	Nominal	1.7 ± 0.1 μm	1.7 ± 0.1 μm
	Through epidermis	2.8 ± 0.8 μm	9.2 ± 1.7 μm
FWHM confocal lateral resolution	Nominal	0.8 ±0.1 μm	1.0 ± 0.1 μm
	Through epidermis	1.6 ± 0.3 μm	1.7 ± 0.1 μm